

Perturbative study of anisotropic lattice actions for heavy quarks

Shoji Hashimoto

High Energy Accelerator Research Organization (KEK), Tsukuba, Ibaraki 305-0801, Japan

Masataka Okamoto

*High Energy Accelerator Research Organization (KEK), Tsukuba, Ibaraki 305-0801, Japan**and Theoretical Physics Department, Fermi National Accelerator Laboratory, P.O. Box 500, Batavia, Illinois 60510, USA*

(Received 22 February 2003; published 12 June 2003)

Anisotropic lattice fermion actions are investigated with one-loop perturbative calculations aiming at constructing a formulation for a heavy quark with controlled systematic uncertainties. For heavy-light systems at rest an anisotropic lattice with small temporal lattice spacing a_t suppresses the discretization error by a power of $a_t m_Q$ for a heavy quark of mass m_Q . We discuss the issue of large discretization errors, which scale as $a_s m_Q$ with a_s the spatial lattice spacing. By performing one-loop calculations of the speed-of-light renormalization for several possible lattice actions in the limit of $a_t \rightarrow 0$, we show that one can eliminate the large systematic error on the anisotropic lattice.

DOI: 10.1103/PhysRevD.67.114503

PACS number(s): 11.15.Ha, 11.10.Gh, 12.38.Bx, 12.38.Gc

I. INTRODUCTION

In heavy quark physics, the lattice simulation of quantum chromodynamics (QCD) is an indispensable tool to compute hadron masses and matrix elements nonperturbatively without introducing model dependence. One of the most important hadron matrix elements in B physics is the B meson decay constant f_B , for which a number of lattice calculations have been performed so far, and the systematic uncertainties are under control at the level of 15% accuracy [1]. In the future, further precise calculations, say better than 5%, are necessary to constrain the Cabibbo-Kobayashi-Maskawa (CKM) matrix elements more strictly and to search for the signature of new physics.

One of the dominant uncertainties in the lattice simulation of heavy quarks is the systematic error associated with the large heavy quark mass, since the lattice cutoff $1/a$ available with current computer power is not much larger than the heavy quark mass m_Q . A conventional approach to avoid this problem is to restrict ourselves to the region where the systematic error is under control ($m_Q \ll 1/a$) and to extrapolate to the b quark mass using the heavy quark scaling law predicted by heavy quark effective theory (HQET). This is unsatisfactory for achieving 5% accuracy, since the possible error scales as $(am_Q)^n$ [$n=2$ for the $O(a)$ -improved action] and thus grows very quickly toward heavier quark masses. Extrapolation to the b quark mass could even amplify the systematic uncertainty.

Another method is the HQET-based approach which includes lattice nonrelativistic QCD (NRQCD) [2,3] and the Fermilab method [4]. In this method one considers the lattice action for the heavy quark as an effective theory valid for large heavy quark masses. The advantage of the HQET-based approach is the absence of the large systematic error which scales as $(am_Q)^n$. The price one has to pay, on the other hand, is the introduction of a number of terms in the action. Their associated coefficients have to be determined by matching the effective theory to the full continuum theory. The matching is usually carried out using perturbation

theory, which limits the accuracy of the lattice calculation.

Besides the HQET-based approach, a possible way to control heavy quark discretization effects is to consider an anisotropic lattice, where the temporal lattice spacing a_t is much smaller than the spatial one a_s [5,6]. Since for a heavy meson (or a heavy baryon) at rest the large energy scale of order m_Q appears only in the temporal component in momentum space, one can expect that the systematic error increases as $(a_t m_Q)^n$ and is therefore suppressed as far as a_t is small enough. The computational cost is not prohibitive if one keeps the spatial lattice spacing relatively large. The problem of the matching of many operators in the effective theory does not appear, as the theory is relativistic.

There is, however, a subtle issue discussed in [7]; for a certain choice of the Wilson term in the spatial direction the systematic error may arise in the combination $a_s m_Q$ rather than the expected $a_t m_Q$ and the virtue of the anisotropic lattice is spoiled. With an alternative choice the error of order $(a_s m_Q)^n$ may be avoided but the unwanted doublers become lighter and disturb the simulation of physical states. The authors of [8] even denied the advantage of the anisotropic lattice used for heavy quarks based on their observation of $a_s m_Q$ -like behavior through radiative corrections. In this paper we discuss this issue further by considering a larger set of $O(a)$ -improved lattice fermion actions and by performing one-loop calculations in the limit $a_t \rightarrow 0$ where no $a_t m_Q$ error remains.

The appearance of large systematic errors scaling as $a_s m_Q$ is naively unexpected for the following reasons. In the $a_t \rightarrow 0$ limit the only source of the discretization error is the spatial derivative in the lattice action. In momentum space, therefore, discretization errors scale as $a_s p$ with p a typical (spatial) momentum scale in the system, which is of order Λ_{QCD} for the heavy-light mesons or baryons at rest, and the combination $a_s m_Q$ may not appear as momentum of order m_Q flows only in the temporal direction. This intuitive picture should be correct even after radiative corrections, because large momentum of order m_Q does not flow in the spatial direction in momentum space, and therefore a dis-

cretization error in the spatial lattice derivative cannot accompany the heavy quark mass m_Q . This becomes clearer if one considers the limit $1/a_s \ll m_Q \ll 1/a_t$, because the spatial momentum integral runs up to π/a_s and thus cannot pick up the larger scale m_Q .

Here, in order to understand the reason why the unexpected $a_s m_Q$ -type error may have appeared in [7,8], let us consider the energy-momentum dispersion relation at the tree level. We consider the $a_t \rightarrow 0$ limit, and the spatial lattice spacing is also kept small enough such that we can neglect errors of $O(a_s^2)$ and higher. For Wilson-type fermions the inverse quark propagator is given by

$$m_Q + i\gamma_0 p_0 + i \sum_i \gamma_i p_i + \frac{r_s}{2\xi} a_s \sum_i p_i^2 + O(a_s^2), \quad (1.1)$$

where r_s denotes the coefficient in front of the spatial Wilson term as defined in Eq. (2.2) in the next section. The term including the anisotropy $\xi = a_s/a_t$ is maintained even in the $a_t \rightarrow 0$ limit, because that term could remain when r_s scales as ξ . To push up the spatial doubler mass in the cutoff scale, r_s/ξ must be kept finite.

The energy-momentum dispersion relation becomes

$$\begin{aligned} -p_0^2 &= \left(m_Q + \frac{r_s}{2\xi} a_s \sum_i p_i^2 \right)^2 + \sum_i p_i^2 + O(a_s^2) \\ &= m_Q^2 + \left(1 + \frac{r_s}{\xi} a_s m_Q \right) \sum_i p_i^2 + O(a_s^2), \end{aligned} \quad (1.2)$$

and thus an error of order $a_s m_Q$ appears unless r_s/ξ vanishes, for which the doublers become light. Since the term $(r_s/\xi)a_s m_Q$ comes from the cross term of the mass and the Wilson terms, the origin of the combination $a_s m_Q$ has nothing to do with the large momentum flow in the spatial direction. At the tree level we may consider a set of lattice actions in which there is no spatial Wilson term by introducing higher derivative operators to decouple the unwanted doublers. This class of action does not have the problem of the $O(a_s m_Q)$ error at the tree level and may be used for heavy quarks even for $a_s m_Q > 1$. There are higher order terms whose coefficient behaves like $a_s m_Q$, but we neglect them as their contribution is $O(a_s^2)$ or higher.

The problem is, then, whether the nice property of these actions is maintained even with radiative corrections. In this paper we perform a one-loop perturbative calculation for these lattice actions and investigate the mass dependence of the rest mass $M_1 = E(\mathbf{0})$ and the kinetic mass $M_2 = (\partial^2 E / \partial p_i^2)_{\mathbf{p}=\mathbf{0}}^{-1}$, where $E(\mathbf{p})$ is the energy of the heavy quark on shell. We examine the functional dependence of the speed-of-light renormalization parameter ν , which is defined such that the relation $M_1 = M_2$ is satisfied. If the one-loop coefficient behaves as $(a_s m_Q)^n$, the action suffers from an unwanted heavy quark mass dependent error. Because we are interested in only the $O((a_s m_Q)^n)$ errors, we carry out the one-loop calculation in the $a_t \rightarrow 0$ limit, where $O((a_s m_Q)^n)$ errors vanish. The fermion actions we consider are the anisotropic SW (Sheikholeslami and Wohlert) action [7,9] and

some special cases of the D234 action [5]. We find the latter to be useful for applications to heavy quark systems.

This paper is organized as follows. In Sec. II, we define the anisotropic fermion actions we consider in this paper and discuss their tree-level properties. The static limit of those actions is considered in Sec. III. The one-loop calculation is then given in Sec. IV, and its results are presented in Sec. V. Section VI is devoted to our conclusions. Some technical details are deferred to the Appendixes.

II. ANISOTROPIC LATTICE FERMION ACTION

We start with the D234 quark action on the anisotropic lattice [5] given by

$$S_{\text{D234}} = a_t a_s^3 \sum_x \bar{\psi}(x) Q \psi(x), \quad (2.1)$$

$$\begin{aligned} Q &= m_0 + \sum_\mu \nu_\mu \gamma_\mu \nabla_\mu (1 - b_\mu a_\mu^2 \Delta_\mu) \\ &\quad \times \frac{1}{2} a_t \left(\sum_\mu r_\mu \Delta_\mu + \sum_{\mu < \nu} c_{\text{SW}}^\mu \sigma_{\mu\nu} F_{\mu\nu} \right) b_f \\ &\quad + \sum_\mu \nu_\mu d_\mu a_\mu^3 \Delta_\mu^2 \end{aligned} \quad (2.2)$$

where $a_0 = a_t$ and $a_i = a_s$ ($i=1,2,3$) are the temporal and spatial lattice spacings, respectively, and

$$(\nu_0, \nu_i) = (1, \nu), \quad (b_0, b_i) = (b_t, b_s), \quad (r_0, r_i) = (r_t, r_s), \quad (2.3)$$

$$(c_{\text{SW}}^0, c_{\text{SW}}^i) = (c_{\text{SW}}^t, c_{\text{SW}}^s), \quad (d_0, d_i) = (d_t, d_s). \quad (2.4)$$

Note that the lattice spacing in front of the Wilson and clover terms is a_t , not a_μ . This notation is similar to the one in [5], but different from those in [6,7]. The anisotropy parameter is defined by

$$\xi \equiv a_s / a_t. \quad (2.5)$$

The lattice covariant derivatives ∇_μ , Δ_μ , $\nabla_\mu \Delta_\mu$, and Δ_μ^2 represent D_μ , D_μ^2 , D_μ^3 , and D_μ^4 , respectively, in the continuum theory, and their detailed definitions are given in Appendix A.

In this paper we always set

$$r_t = 1, \quad b_t = d_t = 0. \quad (2.6)$$

Thus, the operator Q is nothing but the Wilson-Dirac operator as far as the temporal derivatives are concerned. With this condition, the energy-momentum relation for the fermion has a physical solution only, and the unphysical temporal doublers do not appear [5].

Solving $Q(p)Q(p)^\dagger = 0$ in the momentum space and then setting $p_0 = iE$, we obtain the energy-momentum relation for the D234 action as

$$4 \sinh^2\left(\frac{a_t E}{2}\right) = \frac{\nu^2 a_t^2 \sum_i \bar{p}_i^2 (1 + b_s a_i^2 \hat{p}_i^2)^2 + \mu(\mathbf{p})^2}{1 + \mu(\mathbf{p})}, \quad (2.7)$$

where

$$\mu(\mathbf{p}) = a_t m_0 + \frac{1}{2} r_s a_t^2 \sum_i \hat{p}_i^2 + \nu d_s a_t \sum_i a_i^3 \hat{p}_i^4, \quad (2.8)$$

and \bar{p}_μ and \hat{p}_μ are defined in Appendix A.

From Eq. (2.7), we obtain the tree-level rest mass $M_1 = E(\mathbf{0})$ and the kinetic mass $M_2 = (\partial^2 E / \partial p_1^2)_{\mathbf{p}=\mathbf{0}}^{-1}$ as

$$a_t M_1 = \log(1 + a_t m_0), \quad (2.9)$$

$$\frac{1}{a_t M_2} = \frac{2\nu^2}{a_t m_0 (2 + a_t m_0)} + \frac{r_s}{1 + a_t m_0}. \quad (2.10)$$

On the anisotropic lattice with $a_t m_0 \ll 1$, the tree-level mass ratio M_1 / M_2 can be expanded in terms of $a_t m_0$ as

$$M_1 / M_2 = 1 + (r_s - 1) a_t m_0 + O((a_t m_0)^2), \quad (2.11)$$

where we set $\nu = 1$. The deviation of M_1 / M_2 from unity is a lattice discretization error arising from the fermion mass. Unless $r_s \propto \xi$, such an error is a function of $a_t m_0$ alone, which is small on the anisotropic lattice with $a_t m_0 \ll 1$ [7]. When $r_s \propto \xi$, a discretization error of order $a_s m_0 = \xi a_t m_0$ arises, which is still large on the anisotropic lattice.

From Eq. (2.7), we can also calculate the ‘‘spatial-doubler’’ mass E^d , i.e., the energy at the edge of the Brillouin zone ($p_i = \pi/a_s$):

$$a_t E^d = \log \left[1 + a_t m_0 + \frac{2r_s}{\xi^2} n_d + \frac{16\nu d_s}{\xi} n_d \right] \quad (2.12)$$

$$\equiv \log[1 + a_t m_0^d], \quad (2.13)$$

where n_d ($= 1, 2, 3$) is the number of spatial direction with $p_i = \pi/a_s$, and the bare spatial-doubler mass m_0^d is given by

$$a_s m_0^d = a_s m_0 + \frac{2r_s}{\xi} n_d + 16\nu d_s n_d \quad (2.14)$$

in units of the spatial lattice spacing a_s . We note that one has to take $r_s \propto \xi$ or $d_s > 0$ in order to decouple the spatial doubler with energy E^d from the physical state for large values of ξ .

It is interesting to consider the energy-momentum relation in the Hamiltonian limit $a_t \rightarrow 0$ ($\xi \rightarrow \infty$), where $a_t m_0$ errors vanish. In this limit the left-hand side of Eq. (2.7) is replaced by $a_t^2 E^2$, and the energy-momentum relation is simplified to

$$E^2(a_t \rightarrow 0) = \nu^2 \sum_i \bar{p}_i^2 (1 + b_s a_i^2 \hat{p}_i^2)^2 + \frac{\mu(\mathbf{p})^2}{a_t^2} \quad (2.15)$$

$$= m_0^2 + \nu^2 \mathbf{p}^2 + \left(-\frac{\nu^2}{3} + 2\nu^2 b_s + 2a_s m_0 \nu d_s \right) \times a_s^2 \sum_i p_i^4 + O(a^4 p^6). \quad (2.16)$$

From a small \mathbf{p} expansion we obtain a nonrelativistic expression for $E(a_t \rightarrow 0)$:

$$E(a_t \rightarrow 0) = m_0 + \frac{\nu^2}{2m_0} \mathbf{p}^2 - \frac{\nu^4}{8m_0^3} (\mathbf{p}^2)^2 + \frac{1}{2m_0} \left(-\frac{\nu^2}{3} + 2\nu^2 b_s + 2a_s m_0 \nu d_s \right) a_s^2 \sum_i p_i^4 + O(a^5 p^6). \quad (2.17)$$

Taking the static limit $m_0 \rightarrow \infty$ subsequently, one obtains

$$E(a_t \rightarrow 0) \xrightarrow{m_0 \rightarrow \infty} m_0 + \nu d_s a_s^3 \sum_i p_i^4 + O(a^5 p^6). \quad (2.18)$$

Note that the $\sum_i p_i^4$ term survives even in the static limit. This will be discussed later.

We are now ready to define our anisotropic actions more explicitly. We study two actions: one is the SW action [7,9], and the other is a variant of the D234 action [5], which we call the sD34 action. We give these actions and discuss their tree-level properties in the following.

A. SW action

The Sheikholeslami-Wohlert action [7,9] is defined by

$$\nu = r_s = c_{\text{SW}}^\mu = 1, \quad b_s = d_s = 0. \quad (2.19)$$

An $O(a_t)$ error arising from the Wilson terms is removed by $c_{\text{SW}}^\mu = 1$. Since the Wilson terms are $O(a_t)$, this action goes over to the ‘‘naive’’ quark action in the $a_t \rightarrow 0$ ($\xi \rightarrow \infty$) limit. The energy splitting between the physical state and spatial doublers $E^d - E$ vanishes in this limit, as one can find explicitly from Eq. (2.14). The energy-momentum relation for the SW action is shown in Fig. 1. The energy at the edge of the Brillouin zone decreases as ξ increases, which shows the reappearance of the spatial-doubler.

Since $r_s = 1$, the tree-level mass ratio M_1 / M_2 [Eq. (2.11)] contains no $O((a_s m_0)^n)$ error: $M_1 / M_2 = 1 + O((a_t m_0)^2) \xrightarrow{a_t \rightarrow 0} 1$. The anisotropic SW action has been applied to the simulation of charmonium [10] and charmed hadrons [11,12] on $\xi \approx 4$ anisotropic lattices.

B. sD34 action

We define the sD34 action as

$$r_s = c_{\text{SW}}^s = 0, \quad b_s > 0, \quad d_s > 0. \quad (2.20)$$

Although the spatial Wilson term is absent ($r_s = 0$), this action is doubler-free because $d_s > 0$. The energy splitting $E^d - E$ remains even in the $a_t \rightarrow 0$ limit as long as d_s is a con-

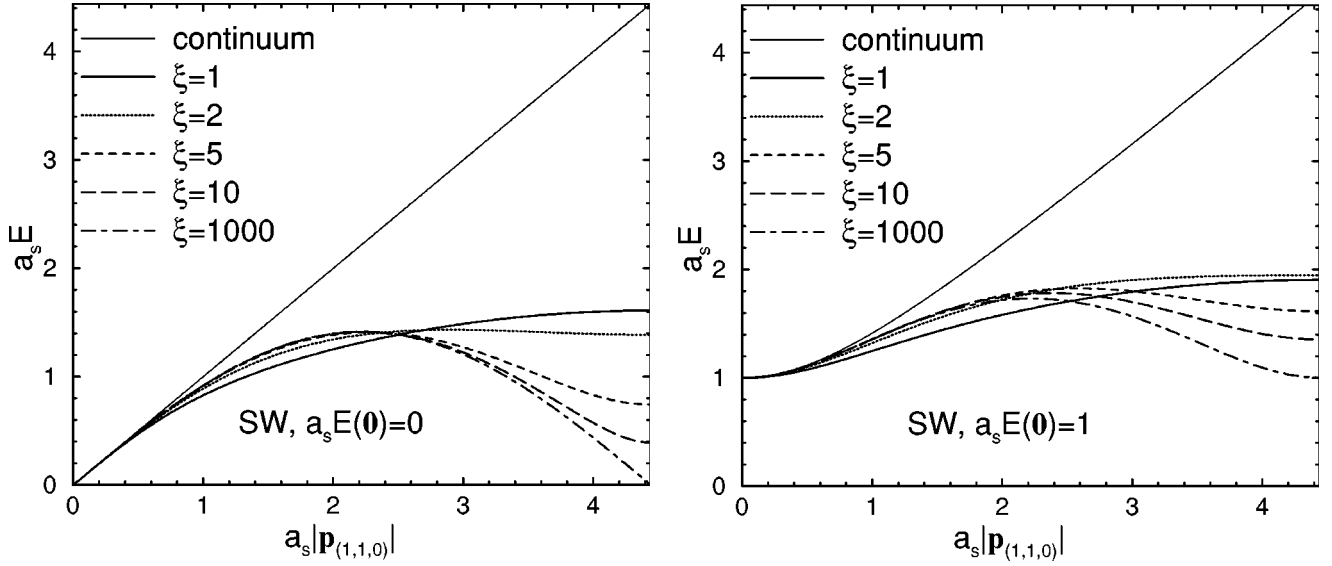


FIG. 1. Energy-momentum relation at different values of ξ for the SW action. The left panel shows the case of $a_s E(\mathbf{0})=0$, while the right shows $a_s E(\mathbf{0})=1$. The spatial momentum \mathbf{p} is along the (1,1,0) direction. For comparison we also plot the energy-momentum relation in the continuum.

stant independent of ξ . Setting $d_s=1/8$ for this action gives the same spatial-doubler mass m_0^d as for the $\xi=1$ SW action when $\nu=1$. The name “sD34” is a reminder that the spatial $\gamma_i D_i^3$ and D_i^4 terms survive in the $a_t \rightarrow 0$ limit. The sD34 action is similar to the one proposed in [13,14], except that those papers considered the case of the isotropic lattice $\xi=1$. Since the sD34 action has next-nearest neighbor interactions such as $\bar{\psi} \nabla_\mu \Delta_\mu \psi$ and $\bar{\psi} \Delta_\mu^2 \psi$, this action is more costly to simulate than the SW action, which consists of the nearest neighbor interactions only.

The sD34 action does not generate $O(a_s)$ discretization errors because $r_s=c_{\text{SW}}^s=0$. In order to remove an $O(a_t)$ error arising from the temporal Wilson term with $r_t=1$, we take

$$\nu=1+\frac{1}{2}r_t a_t m_0, \quad c_{\text{SW}}^t=\frac{1}{2}. \quad (2.21)$$

This condition is obtained by performing a field redefinition $\psi_c=\Omega_c \psi$, $\bar{\psi}_c=\bar{\psi} \bar{\Omega}_c$, $\bar{\Omega}_c=\Omega_c=1-\frac{1}{4}r_t a_t (\mathcal{D}_0-m_c)$ to the continuum quark action $\bar{\psi}_c(x)(\mathcal{D}+m_c)\psi_c(x)$ [5]. Since $r_s=0$ the tree-level mass ratio M_1/M_2 again contains no $O((a_s m_0)^n)$ errors: $M_1/M_2=1+O((a_s m_0)^2) \xrightarrow{a_t \rightarrow 0} 1$.

In the rest of the paper we consider the following three choices of the b_s and d_s parameters:

$$\text{sD34:} \quad b_s=\frac{1}{6}, \quad d_s=\frac{1}{8}, \quad (2.22)$$

$$\text{sD34(v):} \quad b_s=\frac{1}{8}, \quad d_s=\frac{1}{8}, \quad (2.23)$$

$$\text{sD34(p):} \quad b_s=\frac{1}{2}, \quad d_s=\frac{1}{4}. \quad (2.24)$$

The first choice sD34, where $b_s=1/6$, eliminates an $O(a_s^2)$ error arising from the $\gamma_i \nabla_i$ term: $\gamma_i \nabla_i(1-\frac{1}{6}a_s^2 \Delta_i)=\gamma_i D_i+O(a_s^4)$. The second choice sD34(v), where $b_s=1/8$, eliminates an $O(a_s^2)$ error in the one-gluon vertex (A13): $V_{1,i}^a(q,q',k)=-igt^a \gamma_i+O(a_s^3)$. The difference between the one-loop results for sD34 and sD34(v) is numerically small, as shown in the next section. With the third choice sD34(p), the hopping terms in the action are proportional to the projection matrix $1 \pm \gamma_\mu$: using the Wilson projection operator $w_\mu \equiv a_\mu \gamma_\mu \nabla_\mu - \frac{1}{2}a_\mu^2 \Delta_\mu$, the space component of the action is given by $w_i + \frac{1}{2}w_i^2$ ($i=1,2,3$). Therefore the third choice can reduce simulation costs compared to the other two choices [5]. At the tree level the sD34 action (2.22) is $O(a_s^2)$ improved, while the others contain some $O(a_s^2)$ errors. Within the current set of operators (2.2), therefore, the best available choice to suppress discretization effects is the sD34 action.

The energy-momentum relations for the sD34 and sD34(p) actions are shown in Figs. 2 and 3, respectively. For both choices the energy at the edge of the Brillouin zone increases as ξ increases, in contrast to the case of the SW action. In the small $a_s \mathbf{p}$ region, the energy-momentum relation for the sD34 action in Fig. 2 is quite close to the continuum one because it has no $O(a_s^2 \mathbf{p}^2)$ errors. Moreover, in the large $a_s \mathbf{p}$ region near the edge of the Brillouin zone, it is close to the continuum one too, for large values of ξ . From a comparison of Figs. 2 and 3, we expect that the sD34 action can reach the continuum limit faster than the sD34(p) action. We also note that the energy-momentum relation for the sD34(v) action is very similar to that for the sD34 action.

To summarize, neither the SW action nor the sD34 action generates $O((a_s m_Q)^n)$ ($n=1,2,\dots$) errors at the tree level in the mass ratio M_1/M_2 . While the SW action suffers from the spatial doubler for large values of ξ , the sD34 action is doubler-free for any value of ξ . Both actions can be used for

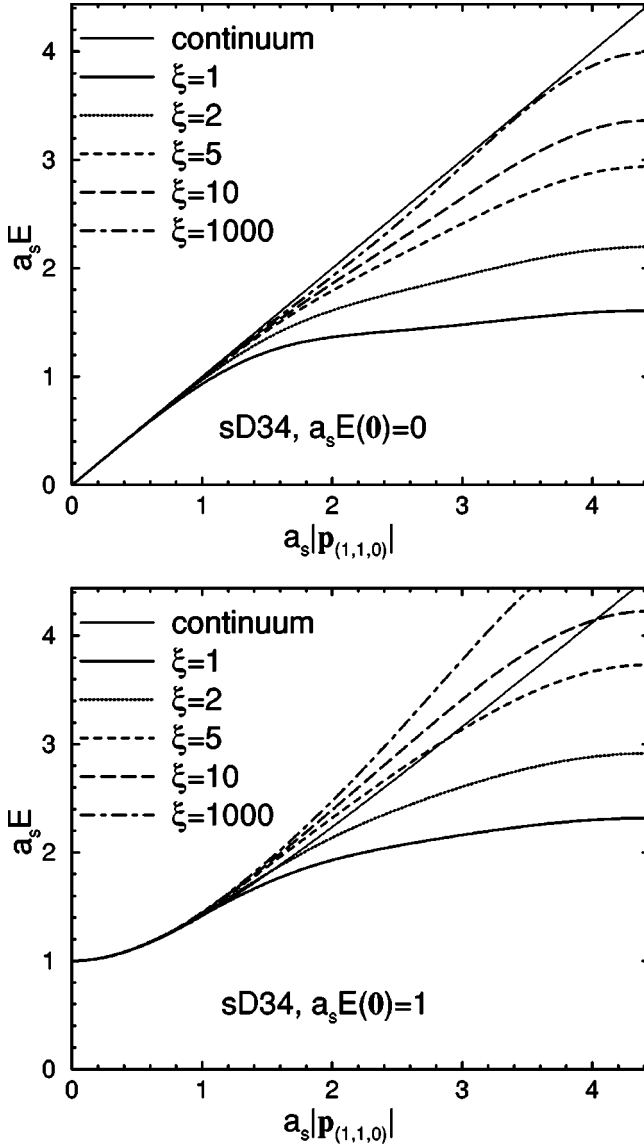


FIG. 2. Energy-momentum relation for the sD34 action.

simulations of the charm quark, if $\xi \approx 2-4$ and $a_t m_c \ll 1$. But simulations of the bottom quark keeping $a_t m_b \ll 1$ require $\xi \approx 5-10$, for which the anisotropic SW action may be contaminated by the spatial doublers.

In addition to the above actions, two other anisotropic actions have been proposed and applied to heavy quark systems: one is the action with $r_t = 1$ and $r_s = \xi$ [6,15–17], and the other is that with $r_t = r_s = \xi$ [18–20]. However, these actions have the spatial Wilson term scaling as $r_s = \xi$ and therefore generate $O((a_s m_0)^n)$ errors in the mass ratio M_1/M_2 even at the tree level when $\nu = 1$, as discussed before and in [7]. For this reason, we do not consider these actions further in this paper.

III. STATIC LIMIT $m_Q \rightarrow \infty$ AND THE HAMILTONIAN LIMIT $a_t \rightarrow 0$

In this section we discuss the static limit $m_Q \rightarrow \infty$ of anisotropic fermion actions. At finite a_t , the action always ap-

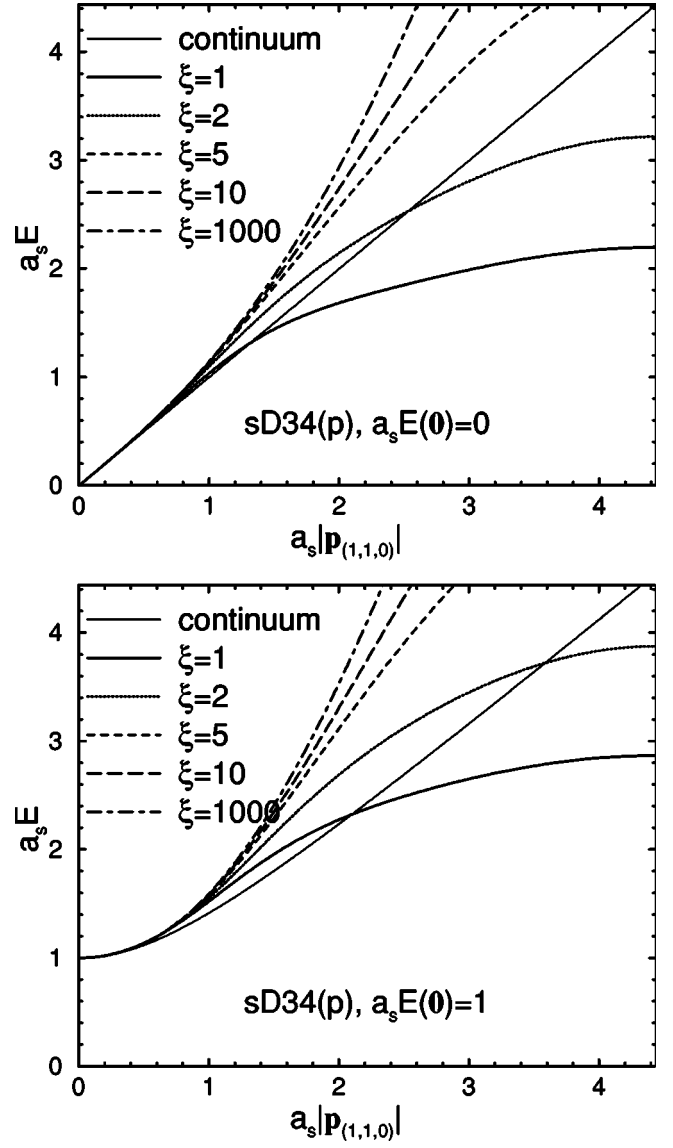


FIG. 3. Energy-momentum relation for the sD34(p) action.

proaches the usual static action in the limit of $a_t m_Q \rightarrow \infty$. This is shown, e.g., by rescaling the fermion field in Eq. (2.1) as

$$\psi(x) = \frac{e^{-a_t M_1 \cdot t}}{\sqrt{a_t m_0}} h(x) \quad (3.1)$$

and then taking $a_t m_0 \rightarrow \infty$.

On the other hand, the action in the limit of $m_Q \rightarrow \infty$ while keeping the condition $a_t m_Q \ll 1$ can be different. In the $a_t \rightarrow 0$ limit, the lattice Dirac operator (2.2) becomes

$$Q(a_t \rightarrow 0) = m_0 + \gamma_0 D_0 + \nu \sum_i \gamma_i \nabla_i (1 - b_s a_i^2 \Delta_i) + \nu d_s a_s^3 \sum_i \Delta_i^2, \quad (3.2)$$

unless $r_s \propto \xi$. Subsequently taking the static limit, the fermion field splits as usual into large and small components in the Dirac representation of the Dirac matrix, and the off-diagonal terms drop out. The action becomes

$$Q(a_t \rightarrow 0) \xrightarrow{m_Q \rightarrow \infty} m_0 + \gamma_0 D_0 + \nu d_s a_s^3 \sum_i \Delta_i^2. \quad (3.3)$$

We note that the $a_s^3 \Delta_i^2$ term, proportional to νd_s , remains in the static limit. The SW action with $d_s=0$ approaches the usual static action, but the sD34 action with $d_s>0$ does not. This observation is consistent with the static energy evaluated in the $a_t \rightarrow 0$ limit (2.18). Formally, the static limit (3.3) can be derived by applying the Foldy-Wouthuysen-Tani transformation

$$\psi(x) \rightarrow \exp\left[-\frac{\nu}{2m_0} \sum_i \gamma_i \nabla_i (1 - b_s a_i^2 \Delta_i)\right] \psi(x) \quad (3.4)$$

to Eq. (3.2) and then taking $m_0 \rightarrow \infty$.

The results of the one-loop calculation at $a_t=0$ in the next section should be consistent with the form (3.3) in the $m_Q \rightarrow \infty$ limit. Suppose that the static action is renormalized as

$$(m_0 + \delta_m) + \gamma_0 D_0 - \frac{1}{2} \delta_r a_s \sum_i \Delta_i + (\nu d_s + \delta_d) a_s^3 \sum_i \Delta_i^2; \quad (3.5)$$

then the mass shift δ_m , the kinetic term renormalization δ_r , and δ_d do not depend on m_0 , but may depend on νd_s because the static propagator and vertices contain νd_s through Eq. (3.3).

IV. ONE-LOOP CALCULATION IN THE HAMILTONIAN LIMIT

In this section we present the one-loop calculations for the anisotropic actions defined in Sec. II. We calculate one-loop corrections to the rest mass and the kinetic mass renormalization factors in the Hamiltonian limit $a_t \rightarrow 0$. From the latter we obtain the one-loop correction to the ν parameter.

A. Formalism

In the one-loop calculation we basically follow the notation of [21] and add some extensions to the case of the anisotropic lattice.

We write the inverse free quark propagator as

$$a_t G_0^{-1}(p) = i a_t \mathbf{K}(p) + a_t L(p) \quad (4.1)$$

and the self-energy as

$$\begin{aligned} a_t \Sigma(p) &= i \sum_{\mu} \gamma_{\mu} A_{\mu}(p) \sin(a_{\mu} p_{\mu}) + C(p) \\ &\equiv i \sum_{\mu} \gamma_{\mu} B_{\mu}(p) + C(p), \end{aligned} \quad (4.2)$$

where p is the external momentum. The inverse full quark propagator is then given by

$$G^{-1}(p) = G_0^{-1}(p) - \Sigma(p). \quad (4.3)$$

Solving $G^{-1}(G^{-1})^{\dagger} = 0$ with $p_0 = iE$, we obtain the all-orders dispersion relation

$$\begin{aligned} 1 + \mu(\mathbf{p}) - \cosh(a_t E) - C \\ = \sqrt{(1 - A_0)^2 \sinh^2(a_t E) - \sum_i [a_t K_i - A_i \sin(a_s p_i)]^2}, \end{aligned} \quad (4.4)$$

where $\mu(\mathbf{p})$ is given in Eq. (2.8).

Setting $\mathbf{p} = \mathbf{0}$ in Eq. (4.4), we obtain the rest mass $M_1 = E(\mathbf{0})$ as

$$\begin{aligned} e^{a_t M_1} &= 1 + a_t m_0 + A_0(iM_1, \mathbf{0}) \sinh(a_t M_1) - C(iM_1, \mathbf{0}) \\ &= 1 + a_t m_0 - iB_0(iM_1, \mathbf{0}) - C(iM_1, \mathbf{0}). \end{aligned} \quad (4.5)$$

In order to have massless quarks remain massless at the quantum level, we need a mass subtraction. Defining the critical bare mass $a_t m_{0c} \equiv C(0, \mathbf{0})$, we can write

$$e^{a_t M_1} = 1 + a_t M_0 - iB_0(iM_1, \mathbf{0}) - C_{\text{sub}}(iM_1, \mathbf{0}), \quad (4.6)$$

where $M_0 = m_0 - m_{0c}$ and $C_{\text{sub}}(iM_1, \mathbf{0}) = C(iM_1, \mathbf{0}) - a_t m_{0c}$. When $M_0 = 0$, the rest mass M_1 vanishes by construction. Usually the mass subtraction is done nonperturbatively in the numerical simulation by defining the critical hopping parameter.

In perturbation theory the rest mass is expanded as

$$M_1 = \sum_{l=0}^{\infty} g^{2l} M_1^{[l]}, \quad (4.7)$$

in which the tree-level rest mass is

$$a_s M_1^{[0]} = \xi \log(1 + a_t M_0) \xrightarrow{a_t \rightarrow 0} a_s M_0, \quad (4.8)$$

while the one-loop coefficient is given by

$$\begin{aligned} a_s M_1^{[1]} &= (-i \xi B_0^{[1]}(iM_1, \mathbf{0}) - \xi C_{\text{sub}}^{[1]}(iM_1, \mathbf{0})) e^{-a_t M_1^{[0]}} \\ &\xrightarrow{a_t \rightarrow 0} -i \xi B_0^{[1]}(iM_1, \mathbf{0}) - \xi C_{\text{sub}}^{[1]}(iM_1, \mathbf{0}). \end{aligned} \quad (4.9)$$

Note that M_1 is now normalized by the spatial lattice spacing a_s . Before the subtraction the one-loop coefficient is given by

$$a_s M_{1, \text{nosub}}^{[1]} \xrightarrow{a_t \rightarrow 0} -i \xi B_0^{[1]}(iM_1, \mathbf{0}) - \xi C^{[1]}(iM_1, \mathbf{0}). \quad (4.10)$$

Differentiating Eq. (4.4) in terms of p_1 twice and then setting $\mathbf{p} = \mathbf{0}$, we obtain the kinetic mass $M_2 = (\partial^2 E / \partial p_1^2)_{\mathbf{p}=\mathbf{0}}^{-1}$ as

$$\frac{e^{a_t M_1} - A_0(iM_1, \mathbf{0}) \cosh(a_t M_1)}{\xi^2 a_t M_2} = \frac{r_s}{\xi^2} + D(\mathbf{0}) + \frac{[\nu/\xi - A_1(iM_1, \mathbf{0})]^2}{[1 - A_0(iM_1, \mathbf{0})] \sinh(a_t M_1)}, \quad (4.11)$$

where

$$\begin{aligned} D(\mathbf{0}) &= \frac{d^2}{d(a_s p_1)^2} [A_0(iE(\mathbf{p}), \mathbf{p}) \sinh(a_t M_1) \\ &\quad - C(iE(\mathbf{p}), \mathbf{p})]_{\mathbf{p}=\mathbf{0}} \\ &= D_{1s}(\mathbf{0}) + \frac{i}{a_s M_2} D_{1t}(\mathbf{0}) + \frac{i}{a_s M_2} \cdot \frac{B_0(iM_1, \mathbf{0})}{\xi \tanh(a_t M_1)} \end{aligned} \quad (4.12)$$

with

$$D_{1s}(\mathbf{0}) = \frac{\partial^2}{\partial(a_s p_1)^2} \left[\frac{1}{i} B_0 - C \right]_{p=(iM_1, \mathbf{0})}, \quad (4.13)$$

$$iD_{1t}(\mathbf{0}) = \frac{\partial}{\partial(a_s p_0)} [B_0 - iC]_{p=(iM_1, \mathbf{0})}. \quad (4.14)$$

The kinetic mass is expanded as

$$M_2 = \sum_{l=0}^{\infty} g^{2l} M_2^{[l]}, \quad (4.15)$$

and the tree-level relation becomes

$$\frac{e^{a_t M_1^{[0]}}}{a_t m_2} = r_s + \frac{\nu^2}{\sinh(a_t M_1^{[0]})} \quad (4.16)$$

where $M_2^{[0]} = m_2(M_1^{[0]})$.

From Eqs. (4.11) and (4.16), we can obtain the kinetic mass renormalization factor defined by

$$Z_{M_2} \equiv \frac{M_2}{m_2(M_1)} = 1 + \sum_{l=1}^{\infty} g^{2l} Z_{M_2}^{[l]}. \quad (4.17)$$

Here the argument of m_2 is the *all-orders* rest mass M_1 . The one-loop coefficient is given by

$$Z_{M_2}^{[1]} = \frac{2\nu\xi A_1^{[1]}(iM_1, \mathbf{0}) - \nu^2 A_0^{[1]}(iM_1, \mathbf{0}) - D^{[1]}(\mathbf{0}) \xi^2 \sinh(a_t M_1)}{\nu^2 + r_s \sinh(a_t M_1)} - A_0^{[1]}(iM_1, \mathbf{0}) \cosh(a_t M_1) e^{-a_t M_1}. \quad (4.18)$$

In the $a_t \rightarrow 0$ limit, the tree-level kinetic mass goes to

$$\frac{1}{m_2} \xrightarrow{a_t \rightarrow 0} \frac{\nu^2}{M_1} + R_s a_s, \quad (4.19)$$

where we defined $R_s \equiv r_s/\xi$, and hence Z_{M_2} goes to

$$Z_{M_2} \xrightarrow{a_t \rightarrow 0} \frac{M_2}{M_1} \nu^2 + R_s a_s M_2. \quad (4.20)$$

Therefore, in this limit, the renormalized ν parameter and R_s , which give $M_1 = M_2$, can be determined from Z_{M_2} :

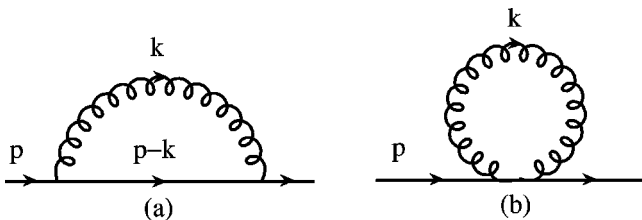


FIG. 4. Feynman graphs relevant for the one-loop quark self-energy. The left (a) is the regular graph, and the right (b) is the tadpole graph.

$$Z_{M_2} \xrightarrow{a_t \rightarrow 0} \nu^2 + R_s a_s M_1 = 1 + (2\nu^{[1]} + R_s^{[1]} a_s M_1^{[0]}) g^2 + O(g^4) \quad (4.21)$$

with the one-loop coefficient

$$Z_{M_2}^{[1]} = 2\nu^{[1]} + R_s^{[1]} a_s M_1^{[0]}. \quad (4.22)$$

Here we used $R_s^{[0]} \rightarrow_{a_t \rightarrow 0} 0$.

On the other hand, from Eq. (4.18) we obtain in this limit

$$\begin{aligned} Z_{M_2}^{[1]} \xrightarrow{a_t \rightarrow 0} & \frac{2}{\nu} \xi A_1^{[1]}(iM_1, \mathbf{0}) - \frac{2}{i} \frac{\xi B_0^{[1]}(iM_1, \mathbf{0})}{a_s M_1} \\ & - a_s m_2 \xi D^{[1]}(\mathbf{0}), \end{aligned} \quad (4.23)$$

where $A_1^{[1]}(iM_1, \mathbf{0}) = [\partial B_1^{[1]}/\partial(a_s p_1)]|_{p=(iM_1, \mathbf{0})}$.

B. One-loop diagrams

Here we compute the one-loop contributions relevant to the rest mass and the kinetic mass renormalization. At the one-loop level, the self-energy is written as

$$\Sigma^{[1]}(p) = \Sigma^{\text{reg}}(p) + \Sigma^{\text{tad}}(p) + \Sigma^{\text{TI}}(p), \quad (4.24)$$

where the contribution from the regular graph Fig. 4(a) is denoted by $\Sigma^{\text{reg}}(p)$, while the tadpole graph Fig. 4(b) gives Σ^{tad} . In order to remove the bulk of Σ^{tad} , we apply the tadpole improvement [22], which amounts to Σ^{TI} . The Feynman rules relevant to our calculations are summarized in Appendix A. We use the anisotropic Wilson gluon action given by

$$S_g = \frac{6}{g^2} \left[\xi \sum_{x,i} [1 - P_{0i}(x)] + \frac{1}{\xi} \sum_{x,i>j} [1 - P_{ij}(x)] \right], \quad (4.25)$$

where $P_{0i}(x)$ and $P_{ij}(x)$ are the temporal and spatial plaquettes, respectively. In the calculations of Σ^{reg} and Σ^{tad} , we adopt the Feynman gauge $\alpha=1$ for the gluon propagator.

C. Regular graph

The contribution from the regular graph is

$$\begin{aligned} a_s \Sigma^{\text{reg}}(p) &= i \sum_{\mu} \gamma_{\mu} \xi B_{\mu}^{\text{reg}}(p) + \xi C^{\text{reg}}(p) \\ &= C_F \int_{-\pi}^{\pi} \frac{d^4 k}{(2\pi)^4} \frac{1}{\xi^2 \hat{k}_0^2 + \hat{\mathbf{k}}^2} \\ &\quad \times \frac{i \sum_{\mu} \gamma_{\mu} \bar{F}_{B\mu}(p, k) + \bar{F}_C(p, k)}{\sum_{\mu} \bar{K}_{\mu}(p-k)^2 + \bar{L}(p-k)^2}, \end{aligned} \quad (4.26)$$

where $\bar{K}_{\mu} = a_t K_{\mu}$, $\bar{L} = a_t L$, the gluon momenta are rescaled as $a_{\mu} k_{\mu} \rightarrow k_{\mu}$ and $a_{\mu} \hat{k}_{\mu} \rightarrow \hat{k}_{\mu}$, and

$$\bar{F}_{B\mu} = a_t F_{B\mu} = 2\bar{K}_{\mu} \bar{X}_{\mu}^2 - \bar{K}_{\mu} \sum_{\rho} (\bar{X}_{\rho}^2 + \bar{Y}_{\rho}^2) + 2\bar{L} \bar{X}_{\mu} \bar{Y}_{\mu}, \quad (4.27)$$

$$\bar{F}_C = a_t F_C = 2 \sum_{\rho} \bar{K}_{\rho} \bar{X}_{\rho} \bar{Y}_{\rho} - \bar{L} \sum_{\rho} (\bar{X}_{\rho}^2 - \bar{Y}_{\rho}^2) \quad (4.28)$$

with $\bar{K}_{\mu} = a_t K_{\mu}(p-k)$, $\bar{L} = a_t L(p-k)$, $\bar{X}_{\mu} = \bar{X}_{\mu}(2p-k, \pm k)$, and $\bar{Y}_{\mu} = \bar{Y}_{\mu}(2p-k, \pm k)$ given in Appendix A. Since the vertices from the clover term $\sigma_{\mu\nu} F_{\mu\nu}$ in the fermion actions are $O(a_t)$ and vanishing in the $a_t \rightarrow 0$ limit, we omit their contributions.

In the $a_t \rightarrow 0$ limit, where

$$F_{B0} \xrightarrow{a_t \rightarrow 0} (p_0 - k_0) \left\{ 1 - \sum_j (\bar{X}_j^2 + \bar{Y}_j^2) \right\}, \quad (4.29)$$

$$F_{Bi} \xrightarrow{a_t \rightarrow 0} 2K_i \bar{X}_i^2 - K_i \left\{ 1 + \sum_j (\bar{X}_j^2 + \bar{Y}_j^2) \right\} + 2L \bar{X}_i \bar{Y}_i, \quad (4.30)$$

$$F_C \xrightarrow{a_t \rightarrow 0} 2 \sum_j K_j \bar{X}_j \bar{Y}_j - L \left\{ 1 + \sum_j (\bar{X}_j^2 - \bar{Y}_j^2) \right\}, \quad (4.31)$$

we obtain

$$\begin{aligned} \xi B_{\mu}^{\text{reg}}(p) &\xrightarrow{a_t \rightarrow 0} \int_{\mathbf{k}} \int_{-\infty}^{\infty} \frac{dk_0}{2\pi} \frac{1}{a_s^2 k_0^2 + \hat{\mathbf{k}}^2} \\ &\quad \times F_{B\mu}(p, k) S_2(p-k), \end{aligned} \quad (4.32)$$

$$\begin{aligned} \xi C^{\text{reg}}(p) &\xrightarrow{a_t \rightarrow 0} \int_{\mathbf{k}} \int_{-\infty}^{\infty} \frac{dk_0}{2\pi} \frac{1}{a_s^2 k_0^2 + \hat{\mathbf{k}}^2} \\ &\quad \times F_C(p, k) S_2(p-k). \end{aligned} \quad (4.33)$$

Here we defined

$$\int_{\mathbf{k}} \equiv C_F \int_{-\pi}^{\pi} \frac{d^3 \mathbf{k}}{(2\pi)^3} \quad (4.34)$$

and

$$S_2(p-k) \equiv \frac{1}{(p_0 - k_0)^2 + \sum_i K_i (p-k)^2 + L(p-k)^2}. \quad (4.35)$$

Differentiating Eqs. (4.32) and (4.33) in terms of the external momenta p and then setting $p = (iM_1, \mathbf{0})$, we obtain the contributions to $M_1^{[1]}$ and $Z_{M_2}^{[1]}$ according to Eqs. (4.9) and (4.23). For the evaluation of the loop integrals, we first integrate over k_0 analytically as described in Appendix B. The remaining integration over \mathbf{k} is evaluated numerically using the adaptive integration routine VEGAS [23].

Since the rest mass and the kinetic mass are physical quantities, the one-loop corrections to them are infrared finite. Although there are infrared divergences in the partial derivatives $D_{1s}(\mathbf{0})$ and $D_{1r}(\mathbf{0})$ in the kinetic mass renormalization, they cancel in the total derivative $D(\mathbf{0})$. In numerical integrations over \mathbf{k} , we evaluate the total derivative directly, rather than evaluating each partial derivative with subtraction of the infrared divergences.

D. Tadpole graph

Although the calculation of Σ^{tad} is much simpler than that of Σ^{reg} , it is worthwhile to show the dependence of the results on the mass and on the parameters. The contribution from the tadpole graph at finite a_t is given by

$$\begin{aligned} a_s \Sigma^{\text{tad}}(p) &= i \sum_{\mu} \gamma_{\mu} \xi B_{\mu}^{\text{tad}}(p) + \xi C^{\text{tad}}(p) \\ &= C_F \int_{-\pi}^{\pi} \frac{d^4 k}{(2\pi)^4} \frac{1}{\xi^2 \hat{k}_0^2 + \hat{\mathbf{k}}^2} \\ &\quad \times \sum_{\mu} \frac{a_{\mu}}{a_t} \left[i \gamma_{\mu} \left\{ a_{\mu} X_{\mu} \sin(a_{\mu} p_{\mu}) \right\} \right] \end{aligned}$$

$$\begin{aligned}
 & + 4a_\mu Z_\mu \sin(2a_\mu p_\mu) \cos^2\left(\frac{k_\mu}{2}\right) \Big\} \\
 & - \left\{ a_\mu Y_\mu \cos(a_\mu p_\mu) + 4a_\mu W_\mu \cos(2a_\mu p_\mu) \right. \\
 & \left. \times \cos^2\left(\frac{k_\mu}{2}\right) \right\}, \tag{4.36}
 \end{aligned}$$

from which we immediately obtain

$$\begin{aligned}
 \xi B_\mu^{\text{tad}}(p) &= C_F \frac{a_\mu}{a_s} \{ J a_\mu X_\mu + 8T_\mu a_\mu Z_\mu \cos(a_\mu p_\mu) \} \\
 & \times \sin(a_\mu p_\mu), \tag{4.37}
 \end{aligned}$$

$$\begin{aligned}
 \xi C^{\text{tad}}(p) &= -C_F \sum_\mu \frac{a_\mu}{a_s} \{ J a_\mu Y_\mu \cos(a_\mu p_\mu) \\
 & + 4T_\mu a_\mu W_\mu \cos(2a_\mu p_\mu) \}, \tag{4.38}
 \end{aligned}$$

where

$$J \equiv \xi \int_{-\pi}^{\pi} \frac{d^4 k}{(2\pi)^4} \frac{1}{\xi^2 \hat{k}_0^2 + \hat{\mathbf{k}}^2}, \tag{4.39}$$

$$T_\mu \equiv \xi \int_{-\pi}^{\pi} \frac{d^4 k}{(2\pi)^4} \frac{1}{\xi^2 \hat{k}_0^2 + \hat{\mathbf{k}}^2} \cos^2\left(\frac{k_\mu}{2}\right). \tag{4.40}$$

In the $a_t \rightarrow 0$ limit, $J = T_0 = 0.2277$ and $T_i = 0.1282$.

The tadpole contributions to $M_1^{[1]}$ and $Z_{M_2}^{[1]}$ in the $a_t \rightarrow 0$ limit are easily calculated from Eqs. (4.37) and (4.38). The contribution to the rest mass before the subtraction (4.10) is given by

$$a_s M_{1,\text{nosub}}^{\text{tad}} \xrightarrow{a_t \rightarrow 0} C_F \sum_i \{ J a_s Y_i + 4T_i a_s W_i \}, \tag{4.41}$$

which depends on $a_s Y_i$ and $a_s W_i$, i.e., νd_s , but not on the mass. It contributes to the critical mass $a_s m_{0c}$ only, so $a_s M_1^{\text{tad}} = 0$ after the subtraction.

The contribution to the kinetic mass renormalization is given by

$$\begin{aligned}
 Z_{M_2}^{\text{tad}} \xrightarrow{a_t \rightarrow 0} & C_F \left[\frac{2}{\nu} (J a_s X_1 + 8T_1 a_s Z_1) + a_s m_2 (J a_s Y_1 \right. \\
 & \left. + 16T_1 a_s W_1) \right]. \tag{4.42}
 \end{aligned}$$

We find that a term proportional to $a_s m_2$ appears, which depends on νd_s again. This manifest $a_s m_Q$ dependence originates from the $\xi D_{(1s)}$ term in Eq. (4.23). Therefore $Z_{M_2}^{\text{tad}}$ diverges as $O(a_s m_Q)$ toward the static limit for the sD34 action with $d_s > 0$, while it is mass independent for the SW

action with $d_s = 0$. Similar mass dependences are also observed in $Z_{M_2}^{\text{reg}}$. We discuss the $O(a_s m_Q)$ divergence of Z_{M_2} in Sec. V.

E. Tadpole improvement

Tadpole improvement [22] is achieved by replacing the link variable U_μ by U_μ/u_μ , where $u_\mu = \langle U_\mu \rangle$ is the mean link variable. In perturbation theory the contribution from the tadpole improvement is obtained from the difference between the inverse free propagator G_0^{-1} and the tadpole-improved inverse free propagator $(G_0^{-1})^{\text{TI}}$ [18]. In momentum space the latter is given by the former with the replacements

$$\begin{aligned}
 \sin(n a_\mu p_\mu) &\rightarrow \sin(n a_\mu p_\mu)/u_\mu^n, \\
 \cos(n a_\mu p_\mu) &\rightarrow \cos(n a_\mu p_\mu)/u_\mu^n, \tag{4.43}
 \end{aligned}$$

where $n = 1, 2, \dots$. The one-loop contribution is then given by

$$\begin{aligned}
 a_s \Sigma^{\text{TI}}(p) &= [a_s G_0^{-1}(p) - a_s (G_0^{-1})^{\text{TI}}(p)]/g^2 \\
 &= \sum_\mu \frac{a_s}{a_\mu} u_\mu^{[1]} [i \gamma_\mu \{ 2a_\mu X_\mu \\
 & + 8a_\mu Z_\mu \cos(a_\mu p_\mu) \} \sin(a_\mu p_\mu) \\
 & - \{ 2a_\mu Y_\mu \cos(a_\mu p_\mu) + 4a_\mu W_\mu \cos(2a_\mu p_\mu) \}], \tag{4.44}
 \end{aligned}$$

where we expanded

$$u_\mu = 1 + g^2 u_\mu^{[1]} + O(g^4) \quad (u_\mu^{[1]} < 0). \tag{4.45}$$

We adopt the mean link in the Landau gauge for the definition of u_μ , which is given by

$$u_\mu^{[1]} = -\frac{1}{2} \frac{a_\mu^2}{a_s^2} C_F J_\mu^{\alpha=0} \tag{4.46}$$

with

$$J_\mu^\alpha = \xi \int_{-\pi}^{\pi} \frac{d^4 k}{(2\pi)^4} \frac{1}{\xi^2 \hat{k}_0^2 + \hat{\mathbf{k}}^2} \left\{ 1 - (1-\alpha) \frac{(a_s^2/a_\mu^2) \hat{k}_\mu^2}{\xi^2 \hat{k}_0^2 + \hat{\mathbf{k}}^2} \right\} \tag{4.47}$$

$$\equiv J - (1-\alpha) \delta J_\mu. \tag{4.48}$$

In the $a_t \rightarrow 0$ limit, $\sum_{i=1}^3 \delta J_i = \delta J_0 = \frac{1}{2} J$. We then obtain

$$\begin{aligned}
 \xi B_\mu^{\text{TI}}(p) &= -C_F \frac{a_\mu}{a_s} J_\mu^{\alpha=0} \{ a_\mu X_\mu + 4a_\mu Z_\mu \cos(a_\mu p_\mu) \} \\
 & \times \sin(a_\mu p_\mu), \tag{4.49}
 \end{aligned}$$

$$\begin{aligned} \xi C^{\text{TI}}(p) = C_F \sum_{\mu} \frac{a_{\mu}}{a_s} J_{\mu}^{\alpha=0} \{ a_{\mu} Y_{\mu} \cos(a_{\mu} p_{\mu}) \\ + 2a_{\mu} W_{\mu} \cos(2a_{\mu} p_{\mu}) \}. \end{aligned} \quad (4.50)$$

Comparing Eqs. (4.49) and (4.50) with Eqs. (4.37) and (4.38), we find that ξB_{μ}^{TI} and ξC_{μ}^{TI} are also obtained from ξB_{μ}^{tad} and ξC_{μ}^{tad} with the replacements

$$J \rightarrow -J_{\mu}^{\alpha=0}, \quad T_{\mu} \rightarrow -\frac{1}{2} J_{\mu}^{\alpha=0}. \quad (4.51)$$

The contributions to $M_{1,\text{nosub}}^{[1]}$ and $Z_{M_2}^{[1]}$ from the tadpole improvement are given by Eqs. (4.41) and (4.42) with the above replacements. Since $J_i^{\alpha=0} = \frac{5}{6} J$, the tadpole contributions are largely canceled by the tadpole improvement.

V. ONE-LOOP RESULTS

A. Rest mass

Now we present the results of our one-loop calculations in the $a_t \rightarrow 0$ limit. The one-loop correction to the rest mass $a_s M_1^{[1]}$ is plotted as a function of $a_s M_1^{[0]}/(1+a_s M_1^{[0]})$ in Fig. 5, and the numerical values of $a_s M_1^{[1]}$ and $a_s m_{0c}^{[1]}$ are given in Table I. As shown in the figure, $a_s M_1^{[1]}$ for all the actions increase from the massless limit and reach their maximum values around $a_s M_1^{[0]} = 1-3$; then decrease to the static values represented by open symbols. By fitting our results in the small mass region ($a_s M_1^{[0]} \ll 1$), we confirmed that the one-loop corrections are consistent with the mass singularity

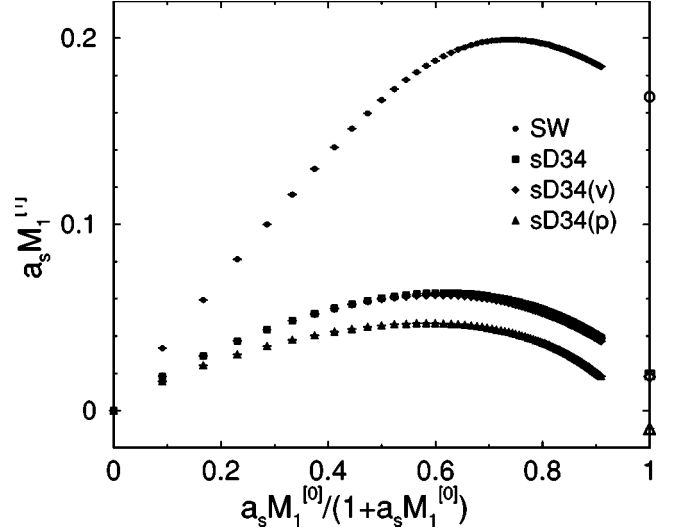


FIG. 5. $a_s M_1^{[1]}$ versus $a_s M_1^{[0]}/(1+a_s M_1^{[0]})$ for the SW action and the sD34 actions. The values in the static limit are denoted by open symbols.

$$M_1^{[1]} \sim -C_F \frac{3}{16\pi^2} M_1^{[0]} \log(a_s M_1^{[0]})^2. \quad (5.1)$$

The results for $a_s M_1^{[1]}$ in the static limit $a_s M_1^{[0]} \rightarrow \infty$ depend on the action, since the reduced static action (3.3) includes the $a_s^3 \Delta_i^2$ term proportional to νd_s . This situation is in contrast to the case of finite a_t calculations in [18,21], where $a_s M_1^{[1]}$ goes to a universal value. In the finite a_t case, $a_s M_1^{[1]}$

TABLE I. Numerical values of $a_s M_1^{[1]}$ for various values of $a_s M_1^{[0]}$, and $a_s m_{0c}^{[1]}$ for the SW action and the sD34 actions.

$a_s M_1^{[0]}$	$a_s M_1^{[1]}$			
	SW	sD34	sD34(v)	sD34(p)
0.0	0.000000(00)	0.000000(00)	0.000000(00)	0.000000(00)
0.1	0.033586(11)	0.018299(19)	0.018360(21)	0.015615(23)
0.2	0.059382(20)	0.029235(21)	0.029306(21)	0.024206(23)
0.3	0.081252(22)	0.037292(24)	0.037354(23)	0.030177(41)
0.4	0.100023(23)	0.043466(28)	0.043405(21)	0.034594(25)
0.5	0.116008(27)	0.048228(29)	0.048196(25)	0.037909(25)
0.6	0.129786(19)	0.051966(24)	0.051762(25)	0.040428(32)
0.7	0.141467(36)	0.054948(34)	0.054572(31)	0.042396(31)
0.8	0.151341(22)	0.057183(24)	0.056763(22)	0.043836(33)
0.9	0.159679(29)	0.059029(36)	0.058465(29)	0.044916(49)
1.0	0.166758(21)	0.060338(33)	0.059687(24)	0.045724(34)
2.0	0.196227(24)	0.062578(35)	0.060997(28)	0.045709(32)
3.0	0.199166(39)	0.058705(39)	0.056713(28)	0.041241(34)
4.0	0.197161(26)	0.054263(23)	0.052280(29)	0.036472(30)
5.0	0.194441(44)	0.050519(28)	0.048617(55)	0.032255(53)
10.0	0.184712(29)	0.038993(46)	0.037121(28)	0.018373(37)
∞	0.168490(26)	0.019045(21)	0.018249(29)	-0.009803(27)
—	0.000000(00)	$a_s m_{0c}^{[1]}$ -0.060828(02)	-0.061672(02)	0.001431(03)

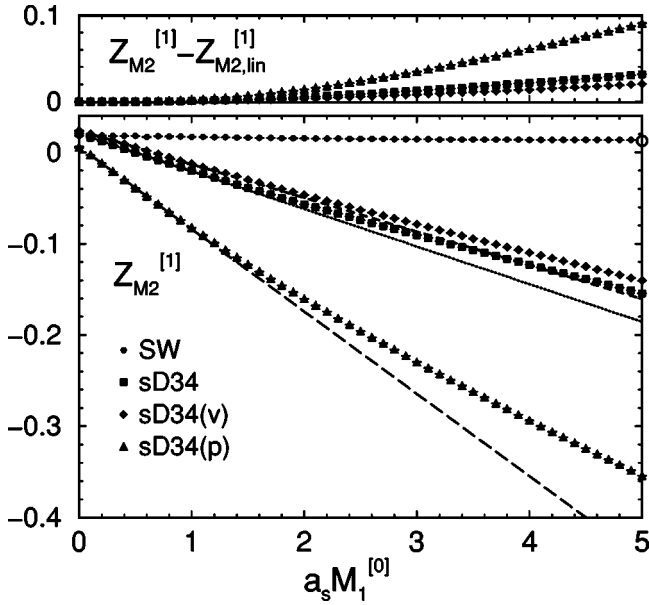


FIG. 6. The lower figure shows $Z_{M_2}^{[1]}$ versus $a_s M_1^{[0]}$ for the SW action and the sD34 actions. The value in the static limit for the SW action is denoted by open circles. Lines are the linear approximations to the results for the sD34 actions ($Z_{M_2,lin}^{[1]}$) as explained in the text. The upper figure shows the difference $Z_{M_2}^{[1]} - Z_{M_2,lin}^{[1]}$ versus $a_s M_1^{[0]}$ for the sD34 actions.

does not depend on νd_s in the $a_s m_Q \rightarrow \infty$ limit, because the static action always gives the Wilson line.

B. Kinetic mass renormalization

The one-loop correction to the kinetic mass renormalization Z_{M_2} is related to the speed-of-light renormalization ν

according to Eq. (4.22). The study of the $a_s m_Q$ dependence of ν at the one-loop level is a main purpose of this paper. The results for $Z_{M_2}^{[1]}$ are shown in Fig. 6, and their numerical values are given in Table II.

First, we focus on the result for the SW action, which becomes the naive quark action in the $a_t \rightarrow 0$ limit as the Wilson term and the clover term vanish. From Fig. 6 (lower panel), we find that the mass dependence of $Z_{M_2}^{[1]}$ (filled circles) is very weak, and $Z_{M_2}^{[1]}$ stays constant in the infinite mass limit. The difference between the value in the static limit and that in the massless limit is $Z_{M_2}^{[1]}(\infty) - Z_{M_2}^{[1]}(0) = -0.006$. This is only 6% of the same difference for the isotropic SW action, -0.10 [21]. The result implies that mass dependent discretization errors of order $g^2(a_s m_Q)^n$ for $Z_{M_2}^{[1]}$ are small on the anisotropic lattice. The same conclusion holds for any action that becomes the naive quark action in the $a_t \rightarrow 0$ limit. For instance, the action with $r_s = 0$ and $d_s = d/\xi$, where d is a constant independent of ξ , belongs to this class. However, we remark that such actions suffer from spatial doublers for large values of ξ , as mentioned in Sec. II.

Next, we consider the results for the sD34 actions, which are doubler-free even in the $a_t \rightarrow 0$ limit. As shown in Fig. 6 (lower panel), $Z_{M_2}^{[1]}$ for the sD34 actions decreases monotonically as the mass increases and diverges as $O(a_s m_Q)$ toward the static limit.

The $O(a_s m_Q)$ divergence of $Z_{M_2}^{[1]}$ is due to the finiteness of $\xi D_{(1s)}$ in the static limit multiplied by $a_s m_2$ in Eq. (4.23). The appearance of this manifest $a_s m_Q$ dependence, which is proportional to νd_s , can be explained as follows. Using $Z_{M_2}^{[1]}$, the kinetic term renormalization δ_r for the static action (3.5) is given by

TABLE II. Numerical values of $Z_{M_2}^{[1]}$ for the SW action and the sD34 actions.

$a_s M_1^{[0]}$	$Z_{M_2}^{[1]}$			
	SW	sD34	sD34(v)	sD34(p)
0.0	0.01810(35)	0.02061(30)	0.02369(49)	0.00549(59)
0.1	0.01812(19)	0.016066(63)	0.020152(61)	-0.00313(11)
0.2	0.018236(53)	0.012019(46)	0.016416(46)	-0.012140(85)
0.3	0.017991(51)	0.007856(48)	0.012592(45)	-0.021208(59)
0.4	0.017941(49)	0.003750(39)	0.009003(38)	-0.030040(78)
0.5	0.017801(43)	-0.000349(34)	0.005406(47)	-0.039223(56)
0.6	0.016708(38)	-0.004308(39)	0.001676(33)	-0.047996(50)
0.7	0.017507(32)	-0.008387(32)	-0.001963(32)	-0.056888(53)
0.8	0.017326(64)	-0.012299(84)	-0.005543(28)	-0.065500(50)
0.9	0.017142(47)	-0.016238(28)	-0.009117(28)	-0.074070(46)
1.0	0.016862(36)	-0.020149(28)	-0.012661(31)	-0.082456(55)
2.0	0.015176(35)	-0.056742(34)	-0.046665(28)	-0.160259(59)
3.0	0.014246(21)	-0.090607(29)	-0.078766(30)	-0.229675(78)
4.0	0.013677(17)	-0.122890(42)	-0.109982(40)	-0.293550(90)
5.0	0.013371(18)	-0.154177(45)	-0.140336(48)	-0.35409(12)
10.0	0.012716(15)	-0.304675(91)	-0.288888(86)	-0.63276(22)
∞	0.012316(07)	$-\infty$	$-\infty$	$-\infty$

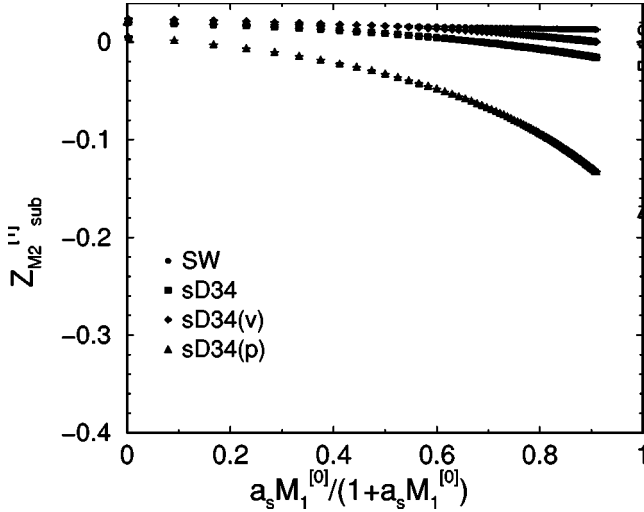


FIG. 7. $Z_{M_2, \text{sub}}^{[1]}$ for the sD34 actions together with $Z_{M_2, \text{sub}}^{[1]} = Z_{M_2}^{[1]}$ for the SW action. The values in the static limit are denoted by open symbols.

$$\delta_r = \lim_{m_Q \rightarrow \infty} \left(\frac{1}{a_s M_2} - \frac{1}{a_s m_2} \right) = - \lim_{m_Q \rightarrow \infty} g^2 \frac{Z_{M_2}^{[1]}}{a_s m_2} + O(g^4). \quad (5.2)$$

Because δ_r is a constant independent of the mass, $Z_{M_2}^{[1]}$ diverges as $O(a_s m_Q)$ in the large mass limit.

However, we note that this kind of $O(a_s m_Q)$ divergence is nothing to do with the discretization error increasing as $a_s m_Q$ but a renormalization of the reduced static action (3.5). In order to isolate such an $O(g^2 a_s m_Q)$ effect, we consider a subtracted $Z_{M_2}^{[1]}$ defined through

$$Z_{M_2, \text{sub}}^{[1]} = Z_{M_2}^{[1]} + \delta_r^{[1]} a_s m_2 \quad (5.3)$$

as a measure of the remaining $O(g^2(a_s m_Q)^n)$ ($n \geq 2$) errors. After the subtraction of the manifest $a_s m_Q$ dependence, $Z_{M_2, \text{sub}}^{[1]}$ for the sD34 actions converges to a finite value in the static limit as shown in Fig. 7. We also find that the mass dependence of $Z_{M_2, \text{sub}}^{[1]}$ for the sD34 and sD34(v) actions is as small as that for the SW action. Note that $Z_{M_2, \text{sub}}^{[1]} = Z_{M_2}^{[1]}$ for the SW action because of $\delta_r = 0$.

Another way to discuss the remaining $O(g^2(a_s m_Q)^n)$ ($n \geq 2$) errors for the sD34 actions is to assess their linearity in the mass parameter. Since $Z_{M_2}^{[1]}$ for the sD34 actions seems to be effectively a linear function of $a_s M_1^{[0]}$ as shown in Fig. 6 (lower panel), we attempt a linear fit using the data for $a_s M_1^{[0]} \leq 0.5$. The fitting lines $Z_{M_2, \text{lin}}^{[1]} = Z_{M_2}^{[1]}(0) + c_r^{[1]} \times a_s M_1^{[0]}$ shown by dashed or dotted lines approximate $Z_{M_2}^{[1]}$ very well from the small mass region $a_s M_1^{[0]} \leq 1$ to the relatively large mass regime $a_s M_1^{[0]} \sim 1$. The difference $Z_{M_2}^{[1]} - Z_{M_2, \text{lin}}^{[1]}$ is plotted in the upper panel of Fig. 6. We find that the difference is less than or about 0.005 (0.01) at $a_s M_1^{[0]} = 1$ (3) for the sD34 and sD34(v) actions, and slightly larger

for the sD34(p) action. Since the (renormalized) coupling constant is $g^2 = 4\pi\alpha_s \sim 2$ in current simulations, the difference from the linearity $g^2(Z_{M_2}^{[1]} - Z_{M_2, \text{lin}}^{[1]})$ is small compared to the tree-level value $Z_{M_2}^{[0]} = 1$. This indicates that $O(g^2(a_s m_Q)^n)$ ($n \geq 2$) errors are suppressed on the anisotropic lattice, and $Z_{M_2}^{[1]}$ for the sD34 actions can be well approximated by a linear ansatz: $Z_{M_2}^{[1]} \approx Z_{M_2, \text{lin}}^{[1]}$.

If one would like to avoid the appearance of the renormalization scaling as $a_s m_Q$, it is possible to tune the spatial Wilson term as $R_s^{[1]} = -\delta_r^{[1]}$ such that the second term in Eq. (5.3) vanishes, and then the one-loop coefficient of the speed-of-light renormalization is given by $\nu^{[1]} = Z_{M_2, \text{sub}}^{[1]}/2$. Since the remaining $O((a_s m_Q)^n)$ correction for $\nu^{[1]}$ is small and does not diverge as a function of $a_s m_Q$ as shown in Fig. 7, it essentially solves the problem of the large radiative correction in the anisotropic lattice actions for the heavy quark. It also suggests that if one can nonperturbatively tune the Wilson term in the static limit, e.g. by adjusting r_s until the $O(a_s m_Q)$ divergence of Z_{M_2} for mesons disappears, the above cancellation of the $a_s m_Q$ error can be implemented nonperturbatively.

VI. CONCLUSIONS

In this paper we discuss on the issue whether the discretization error scales as $(a_s m_Q)^n$ when the heavy quark action is discretized on an anisotropic lattice for which the temporal lattice spacing a_t is very small in order to keep the condition $a_t m_Q \ll 1$, while the spatial lattice spacing a_s is relatively large and $a_s m_Q$ can be of order 1. Our naive expectation is that the discretization error does not behave as $a_s m_Q$ for heavy-light mesons (or baryons) at rest, since the momentum scale flowing in the spatial direction is of order of the QCD scale Λ_{QCD} rather than the heavy quark mass scale m_Q . Even at the quantum level the maximum (virtual) momentum flowing into the spatial direction is π/a_s , and the discretization error coming from the spatial derivative cannot pick up the large heavy quark mass.

Through one-loop calculations of the kinetic mass renormalization for a class of lattice fermion actions, we found that our expectation is indeed met. For the sD34 actions there is a piece that behaves as $a_s m_Q$ in the one-loop coefficient of the kinetic mass renormalization, but it originates from the renormalization of the spatial Wilson term, which remains even in the static limit, and thus does not come from the discretization of the spatial derivative. This implies that if one can nonperturbatively tune the spatial Wilson term (the parameter r_s) such that it vanishes in the static limit, the unwanted behavior $a_s m_Q$ can be removed from the speed-of-light renormalization. Although there is the possibility that the unwanted discretization error scaling as $a_s m_Q$ exists in some other quantities, it is unlikely from our considerations.

The anisotropic lattice thus remains a promising approach to treat heavy quarks on the lattice. As in the usual relativistic approach, the theory is renormalizable and the number of necessary terms in the action is limited. It also opens the

possibility of tuning the parameters in the action nonperturbatively for heavy quarks.

ACKNOWLEDGMENTS

We thank Tetsuya Onogi, Shinichi Tominaga, and Norikazu Yamada for useful discussions. We also thank Andreas Kronfeld for carefully reading the manuscript. This work is supported in part by Grants-in-Aid of the Ministry of Education under Contract No. 14540289. M.O. is also supported by the JSPS.

APPENDIX A: DEFINITIONS AND FEYNMAN RULES

The lattice covariant derivatives are defined by

$$\nabla_\mu \psi(x) \equiv \frac{1}{2a_\mu} [U_\mu(x) \psi(x+\mu) - U_{-\mu}(x) \psi(x-\mu)], \quad (\text{A1})$$

$$\Delta_\mu \psi(x) \equiv \frac{1}{a_\mu^2} [U_\mu(x) \psi(x+\mu) + U_{-\mu}(x) \psi(x-\mu) - 2\psi(x)], \quad (\text{A2})$$

$$\begin{aligned} \nabla_\mu \Delta_\mu \psi(x) \equiv & \frac{1}{2a_\mu^3} [U_\mu(x) U_\mu(x+\mu) \psi(x+2\mu) \\ & - U_{-\mu}(x) U_{-\mu}(x-\mu) \psi(x-2\mu) \\ & - 2U_\mu(x) \psi(x+\mu) + 2U_{-\mu}(x) \psi(x-\mu)], \end{aligned} \quad (\text{A3})$$

$$\begin{aligned} \Delta_\mu^2 \psi(x) \equiv & \frac{1}{a_\mu^4} [U_\mu(x) U_\mu(x+\mu) \psi(x+2\mu) \\ & + U_{-\mu}(x) U_{-\mu}(x-\mu) \psi(x-2\mu) \\ & - 4U_\mu(x) \psi(x+\mu) - 4U_{-\mu}(x) \psi(x-\mu) \\ & + 6\psi(x)]. \end{aligned} \quad (\text{A4})$$

We also define the lattice momenta

$$a_\mu \bar{p}_\mu \equiv \sin(a_\mu p_\mu), \quad (\text{A5})$$

$$a_\mu \hat{p}_\mu \equiv 2 \sin(a_\mu p_\mu/2). \quad (\text{A6})$$

The Feynman rules for our anisotropic actions can be derived in the usual way. The gluon propagator in the Feynman gauge is given by

$$D_{\mu\nu}^{ab}(k) = \frac{\delta^{ab} \delta_{\mu\nu}}{\hat{k}^2}. \quad (\text{A7})$$

The quark propagator is

$$G_0(p) = \frac{1}{i \sum_\mu \gamma_\mu K_\mu(p) + L(p)}, \quad (\text{A8})$$

where

$$K_0(p) = \bar{p}_0 \xrightarrow{a_t \rightarrow 0} p_0, \quad (\text{A9})$$

$$K_i(p) = v \bar{p}_i (1 + b_s a_i^2 \hat{p}_i^2), \quad (\text{A10})$$

and

$$L(p) = m_0 + \frac{1}{2} a_t \sum_\mu r_\mu \hat{p}_\mu^2 + v d_s \sum_i a_i^3 \hat{p}_i^4 \quad (\text{A11})$$

$$\xrightarrow{a_t \rightarrow 0} m_0 + v d_s \sum_i a_i^3 \hat{p}_i^4 \quad (\text{A12})$$

for our quark actions with Eq. (2.6).

The one-gluon vertex with incoming quark momentum q , outgoing quark momentum q' , and incoming gluon momentum $k = q' - q$ is given by

$$V_{1,\mu}^a(q, q', k) = -igt^a [\gamma_\mu \bar{X}_\mu(q + q', k) - i\bar{Y}_\mu(q + q', k)], \quad (\text{A13})$$

where

$$\begin{aligned} \bar{X}_\mu(q + q', k) = & 2a_\mu X_\mu \cos\left(\frac{a_\mu q_\mu + a_\mu q'_\mu}{2}\right) \\ & + 4a_\mu Z_\mu \cos(a_\mu q_\mu + a_\mu q'_\mu) \cos\left(\frac{a_\mu k_\mu}{2}\right), \end{aligned} \quad (\text{A14})$$

$$\begin{aligned} \bar{Y}_\mu(q + q', k) = & 2a_\mu Y_\mu \sin\left(\frac{a_\mu q_\mu + a_\mu q'_\mu}{2}\right) \\ & + 4a_\mu W_\mu \sin(a_\mu q_\mu + a_\mu q'_\mu) \cos\left(\frac{a_\mu k_\mu}{2}\right), \end{aligned} \quad (\text{A15})$$

and

$$a_\mu X_\mu = \frac{1}{2} v_\mu + v_\mu b_\mu, \quad (\text{A16})$$

$$a_\mu Y_\mu = \frac{1}{2} r_\mu \frac{a_0}{a_\mu} + 4v_\mu d_\mu, \quad (\text{A17})$$

$$a_\mu Z_\mu = -\frac{1}{2} v_\mu b_\mu, \quad (\text{A18})$$

$$a_\mu W_\mu = -v_\mu d_\mu. \quad (\text{A19})$$

The t^a are generators of color SU(3). We ignore the one-gluon vertex arising from the clover terms because this vertex becomes irrelevant in the $a_t \rightarrow 0$ limit.

Finally, the two-gluon vertex with incoming gluon momenta k and k' ($k+k'=q'-q$) is given by

$$\begin{aligned}
V_{2,\mu\mu}^{ab}(q,q',k,k') &= 2a_\mu g^2 (t^a t^b) \\
&\times \left[i\gamma_\mu \left\{ a_\mu X_\mu \sin\left(\frac{a_\mu q_\mu + a_\mu q'_\mu}{2}\right) \right. \right. \\
&\quad + 4a_\mu Z_\mu \sin(a_\mu q_\mu \\
&\quad \left. \left. + a_\mu q'_\mu) \cos\left(\frac{a_\mu k_\mu}{2}\right) \cos\left(\frac{a_\mu k'_\mu}{2}\right) \right\} \right. \\
&\quad - \left\{ a_\mu Y_\mu \cos\left(\frac{a_\mu q_\mu + a_\mu q'_\mu}{2}\right) \right. \\
&\quad + 4a_\mu W_\mu \cos(a_\mu q_\mu \\
&\quad \left. \left. + a_\mu q'_\mu) \cos\left(\frac{a_\mu k_\mu}{2}\right) \cos\left(\frac{a_\mu k'_\mu}{2}\right) \right\} \right]. \tag{A20}
\end{aligned}$$

Here we omit terms that vanish by symmetrizing between two gluons and that arise from the clover terms, which are unnecessary in the calculation of the tadpole graph.

APPENDIX B: k_0 INTEGRATIONS

In this appendix we summarize some formulas for the k_0 integrations, which are needed for the calculation of the regular graph. We use the following results for one-dimensional integrations:

$$\begin{aligned}
I_1 &\equiv \int_{-\infty}^{\infty} dx \frac{1}{a+bx^2} \frac{c}{g^2(ie-x)^2+f^2} \\
&= \pi c \left\{ \frac{1}{\sqrt{ab}} \frac{1}{-g^2(e-\sqrt{a/b})^2+f^2} + \frac{1}{a-b(e+f/g)^2} \frac{1}{fg} \right\}, \tag{B1}
\end{aligned}$$

$$\begin{aligned}
I_2 &\equiv \int_{-\infty}^{\infty} dx \frac{1}{a+bx^2} \frac{c(ie-x)}{g^2(ie-x)^2+f^2} \\
&= i\pi c \left\{ \frac{1}{\sqrt{ab}} \frac{e-\sqrt{a/b}}{-g^2(e-\sqrt{a/b})^2+f^2} - \frac{1}{a-b(e+f/g)^2} \frac{1}{g^2} \right\}, \tag{B2}
\end{aligned}$$

$$I_3 \equiv \int_{-\infty}^{\infty} dx \frac{1}{a+bx^2} \frac{c}{(g^2(ie-x)^2+f^2)^2} = -\frac{1}{2f} \frac{\partial I_1}{\partial f}, \tag{B3}$$

$$I_4 \equiv \int_{-\infty}^{\infty} dx \frac{1}{a+bx^2} \frac{c(ie-x)^2}{(g^2(ie-x)^2+f^2)^2} = -\frac{1}{2g} \frac{\partial I_1}{\partial g}, \tag{B4}$$

$$I_5 \equiv \int_{-\infty}^{\infty} dx \frac{1}{a+bx^2} \frac{c(ie-x)}{(g^2(ie-x)^2+f^2)^2} = -\frac{1}{2f} \frac{\partial I_2}{\partial f}, \tag{B5}$$

$$I_6 \equiv \int_{-\infty}^{\infty} dx \frac{1}{a+bx^2} \frac{c}{(g^2(ie-x)^2+f^2)^3} = -\frac{1}{4f} \frac{\partial I_3}{\partial f}, \tag{B6}$$

$$I_7 \equiv \int_{-\infty}^{\infty} dx \frac{1}{a+bx^2} \frac{c(ie-x)}{(g^2(ie-x)^2+f^2)^3} = -\frac{1}{4f} \frac{\partial I_5}{\partial f}, \tag{B7}$$

where $e < f/g$ is assumed. These integrations are calculated by hand using the residue theorem and checked by MATHEMATICA.

In the calculation of the regular graph, we assign

$$\begin{aligned}
x &\rightarrow k_0, \quad a \rightarrow |\hat{\mathbf{k}}|^2, \quad b \rightarrow a_s^2, \quad g \rightarrow 1, \quad e \rightarrow M_1, \\
f &\rightarrow E(\mathbf{k}), \tag{B8}
\end{aligned}$$

where

$$E(\mathbf{k}) \equiv \sqrt{\nu^2 \sum_i \bar{k}_i^2 (1 + b_s a_i^2 \hat{k}_i^2)^2 + \left(m_0 + \nu d_s \sum_i a_i^3 \hat{k}_i^4 \right)^2}. \tag{B9}$$

The overall factors c depend on the spatial momentum \mathbf{k} . Using the integrations I_1 – I_7 with the above assignments, the relevant contributions from the regular graph are given by

$$\xi B_0^{\text{reg}}(iM_1, \mathbf{0}) = \int_{\mathbf{k}} \frac{1}{2\pi} I_{2-B0}, \tag{B10}$$

$$\xi C^{\text{reg}}(iM_1, \mathbf{0}) = \int_{\mathbf{k}} \frac{1}{2\pi} I_{1-C}, \tag{B11}$$

$$\xi A_1^{\text{reg}}(iM_1, \mathbf{0}) = \int_{\mathbf{k}} \frac{1}{2\pi} (I_{1-A1} + I_{3-A1}), \tag{B12}$$

$$\begin{aligned}
\xi D_{1s}^{\text{reg}}(\mathbf{0}) &= \int_{\mathbf{k}} \frac{1}{2\pi} \left[\frac{1}{i} (I_{2-Ds} + I_{5-Ds} + I_{7-Ds}) \right. \\
&\quad \left. - (I_{1-Ds} + I_{3-Ds} + I_{6-Ds}) \right], \tag{B13}
\end{aligned}$$

$$i \xi D_{1t}^{\text{reg}}(\mathbf{0}) = \int_{\mathbf{k}} \frac{1}{2\pi} (I_{1-Dt} + I_{4-Dt} - i I_{5-Dt}). \tag{B14}$$

- [1] N. Yamada, review talk at 20th International Symposium on Lattice Field Theory (LATTICE 2002), Boston, Massachusetts, 2002, hep-lat/0210035.
- [2] B. A. Thacker and G. P. Lepage, Phys. Rev. D **43**, 196 (1991).
- [3] G. P. Lepage, L. Magnea, C. Nakhleh, U. Magnea, and K. Hornbostel, Phys. Rev. D **46**, 4052 (1992).
- [4] A. X. El-Khadra, A. S. Kronfeld, and P. B. Mackenzie, Phys. Rev. D **55**, 3933 (1997).
- [5] M. G. Alford, T. R. Klassen, and G. P. Lepage, Nucl. Phys. **B496**, 377 (1997).
- [6] T. R. Klassen, Nucl. Phys. B (Proc. Suppl.) **73**, 918 (1999); and (unpublished).
- [7] J. Harada, A. S. Kronfeld, H. Matsufuru, N. Nakajima, and T. Onogi, Phys. Rev. D **64**, 074501 (2001).
- [8] S. Aoki, Y. Kuramashi, and S. Tominaga, Prog. Theor. Phys. **109**, 383 (2003).
- [9] B. Sheikholeslami and R. Wohlert, Nucl. Phys. **B259**, 572 (1985).
- [10] T. Umeda, R. Katayama, O. Miyamura, and H. Matsufuru, Int. J. Mod. Phys. A **16**, 2215 (2001).
- [11] H. Matsufuru, T. Onogi, and T. Umeda, Phys. Rev. D **64**, 114503 (2001).
- [12] J. Harada, H. Matsufuru, T. Onogi, and A. Sugita, Phys. Rev. D **66**, 014509 (2002).
- [13] H. W. Hamber and C. M. Wu, Phys. Lett. **133B**, 351 (1983).
- [14] T. Eguchi and N. Kawamoto, Nucl. Phys. **B237**, 609 (1984).
- [15] P. Chen, Phys. Rev. D **64**, 034509 (2001).
- [16] CP-PACS Collaboration, M. Okamoto *et al.*, Phys. Rev. D **65**, 094508 (2002).
- [17] Z. H. Mei and X. Q. Luo, hep-lat/0206012.
- [18] S. Groote and J. Shigemitsu, Phys. Rev. D **62**, 014508 (2000).
- [19] UKQCD Collaboration, S. Collins, C. T. Davies, J. Hein, R. R. Horgan, G. P. Lepage, and J. Shigemitsu, Phys. Rev. D **64**, 055002 (2001).
- [20] J. Shigemitsu, S. Collins, C. T. Davies, J. Hein, R. R. Horgan, and G. P. Lepage, Phys. Rev. D **66**, 074506 (2002).
- [21] B. P. Mertens, A. S. Kronfeld, and A. X. El-Khadra, Phys. Rev. D **58**, 034505 (1998).
- [22] G. P. Lepage and P. B. Mackenzie, Phys. Rev. D **48**, 2250 (1993).
- [23] G. P. Lepage, J. Comput. Phys. **27**, 192 (1978).